Global Journal of Earth and Environmental Science
Volume 9(4), pages 157-170, December 2024
Article Number: B42948844
ISSN: 2636-6002
https://doi.org/10.31248/GJEES2024.170
https://integrityresjournals.org/journal/GJEES
Full Length Research

Identification of hydrothermal alteration mapping using spectral analysis of ASTER Data in NE Tohamiyam Area, Red Sea Hills, NE Sudan

Adam Alsaid Blila Mohammed[1], Sami Omer Hag El Khidir[2], Dafalla Wadi[4] and Mohammed Ishag Abdallsamed[3]*

[1]Regional Geology Administration, Geological Research Authority of Sudan (GRAS), Ministry of Minerals, Khartoum, 410, Sudan.
[2]Department of Geology, Faculty of Petroleum and Minerals, Al Neelain University, 52nd St, Khartoum, 12702, Sudan.
[3]Department of Geology, Faculty of Science, University of Kordofan, B160, Elobeid, Sudan.
[4]Department of Hydrogeology and Engineering Geology, college of Petroleum Geology and Minerals, University of Bahri, P. O. Box 2469, Khartoum–Sudan.

*Corresponding author. Email: mabdallsamed.geo@gmail.com; Tel: +249123203919.

Received 28th November 2024; Accepted 26th December 2024

ABSTRACT: The Tohamiyam area is located in the Red Sea Hills in East Sudan. Remote Sensing and GIS investigations were carried out in the study area using the ASTER data on VNIR and SWIR in mineral prospecting. It has increased recently because of its relatively low cost, broad coverage, and unique integral bands, susceptible to alteration minerals. The study aimed to delineate the hydrothermal alteration zones related to mineralization. The area is a part of the Haiya terrane (HT) of the late Proterozoic Arabian-Nubian Shield (ANS). The Haiya terrain consists predominantly of arc-back arc low-grade metavolcanic-sedimentary sequences decorated with dismembered ophiolitic rocks and intruded by granitoid intrusions of different ages. The ASTER semi-hyperspectral data have been treated with a Mixture Tuned Matched Filtering (MTMF) classifier. The MTMF classifier matches the spectral signatures of the indicator minerals with similar spectra from the ASTER–USGS spectral library. MTMF classifier images portrayed at least many sites as highly probable alteration mineralization zones in the NE part of the study area, which conforms with the results obtained from Aster data. This study revealed that the results of mineral prospecting investigations obtained from ASTER data show that they can distinguish the spectral signatures of the indicator minerals and delineate the alteration halos related to mineralization zones. The results of remote sensing applications with field geochemical data show that the spectral and spatial analysis of optical semi-hyperspectral data in mineral exploration investigations is strengthened. This study recommends remote sensing and machine learning technology in mineral studies through hydrothermal alteration within the basement complex rocks of the Nubian Shield in Red Sea hills.

Keywords: Alternations, ASTER, hydrothermal, identification, mapping, remote sensing, spectrum analysis.

INTRODUCTION

The Red Sea Hills (RSH) is an extending regional topographic feature in Egypt, Sudan, Eretria, Ethiopia, Saudi Arabia, and Yemen. The RSH formed due to the late Proterozoic East African Orogen, which was later split by rifting and the formation of the Red Sea. The RSH has been well known as one potential mineralization terrain worth mentioning; Sudan mineral deposits, such as gold, copper, iron, chrome, etc., are of significant economic value and are associated with mountainous terrains. The rigid topography, harsh environment, and lack of good

infrastructure in the RSH hindered the development of the mining industry. This is because the development and sustainability of any region largely depend on the availability of natural resources and how they are utilized. In order to achieve development and sustainability, harnessing these natural resources, such as mineral resources, is necessary. This can be achieved through systematic prospecting and exploration programs to utilize the natural resources sustainably). Hence, remote sensing as a science, technique, and methodology proved valuable for many geological fields, specifically the regional geological mapping, prospecting, and exploration of suitable mineral deposits and water resources. In Sudan, many types of research involving optical and radar remote sensing data have been conducted for geological mapping and mineral exploration (Babikii, 2006; El Khidir, 2006; El Khidir and Babikir, 2013; Ali, 2005; Elsayed Zeinelabdein, 2002; Kenea, 1997; Abdelsalam *et al.,* 1995; Wadi *et al*., 2021; Saad *et al.,* 2024).

Over the past fifteen years, researchers have become increasingly interested in the use of satellite imagery for activities related to mine exploration, as it has provided important results, especially hyper- and multispectral imagery such as the Advanced Spaceborne Thermal Emission and Reflection Radiometer (ASTER), which was launched in December 1999. This program collects surface data with fourteen bands in different spectral ranges: three bands in the visible and near-infrared range, six in the mid-infrared range, and five in the thermal range (Honarmand *et al*., 2013). The mid-infrared and thermal bands have proven to be the most useful in assessing geological resources and identifying areas of epithermal and hydrothermal alteration (Mohammed and El Khidir, 2023; Chen *et al*., 2022; Testa *et al*., 2018; Rajendran and Nasir, 2017; Pour and Hashim, 2012).

Mixture Tuned Matched Filtering (MTMF) is an advanced matched-filtering technique that reduces false positives. It can be seen as a combination of the statistical matched filtering model with the linear spectral unmixing model (Siddiqui *et al.,* 2022). MTMF is considered extremely useful for detecting target materials where knowledge of the background material is eliminated (Boardman and Kruse 2011; Mehr *et al*., 2013). Targets with low spectral contrast between target and background and within targets can also be detected using the specialized method of MTMF.

The study area lies in NE Tohamiyam town and the railway station in the Red Sea Hills. Administratively, the area lies within the boundaries of the Haiya area in the Red Sea State. Geographically, the area under consideration is mapped within the Sinkat topo-sheet (NE-37-E-Sinkat; scale 250K), bounded by longitudes 36°37’22.88”-36°52’41.59”E and latitudes 18°47’1.86”- 18°29’26.09”N. The main towns in the study area are Haiya, Tohamiyam, and Summit. Haiya town lies at the junction of two highways that can be accessed via the national highway network, which connects Khartoum (Sudan's capital) and Port Sudan (The main port). Therefore, the area can be accessed by the main national highway road connecting Khartoum- Atbara- Haiya- Port Sudan (800-Km), while the second national highway road connects Khartoum-Wad Medani- Gedarif-Kassala-Haiya-Port Sudan (1200-Km). The railway runs parallel to the first highway road. Regular daily flights run between Khartoum and Port Sudan. (Figure 1).

GEOLOGY AND TECTONIC SETTING

The Red Sea Hills “RSH” represents the western part of the Arabian-Nubian Shield “ANS,” which is dominated by the arc and back-arc metavolcanic-sedimentary sequences decorated by mafic-ultramafic ophiolitic sutures formed by Pan-African orogeny in the Neoproterozoic age (Vail, 1979). The Sudanese RSH region occupies a central position in the Nubian segment of the ANS. These hills constitute a semi-desert plateau of mountains no more than 200 km wide and rising to 2000-m (*a. m. s. l*.). The mafic-ultramafic ophiolite complexes represent suture zones along which oceans and back-arc basins have closed (Fitches *et al*., 1983; Vail, 1983). Moreover, they were probably continuous with their equivalents on the Arabian side of the ANS (Vail, 1985; Camp, 1984; Bakor *et al*., 1976). The geological studies in NE Sudan started in the early 1950s; in 1976, Vail attempted to integrate the Red Sea Hills into the geology of the entire ANS (Vail *et al*., 1976). Further subsequent work led to a first evolutionary model for the region, whereby three separate crustal entities were identified, each reflecting temporally distinct cycles of magmatic activity separated by ophiolite belts (Vail, 1983; Vail, 1985). Others supported the arc accretion model developed for the Eastern Desert of Egypt and Western Arabia based on the remarkable similarity of rock types and their tectonic setting with those of NE Sudan (Neary *et al*., 1976). This region has been correlated with adjacent areas in NE Africa and divided into two major geodynamic systems, namely gneisses with interfolded supracrustal metasediments and a dominantly low-grade juvenile ophiolitic island-arc assemblage (Abdel Rahman, 1993). The Precambrian basement complex of RSH is divided into three major lithological units; these three lithological units are:

1. High-grade gneisses, formerly known as (the Kashabib series), represent the roots of the arc assemblages.
2. Low-grade volcano-sedimentary sequence, formerly named (Nafirdeib Series).
3. 3- A more differentiated, less metamorphosed volcano-sedimentary sequence, formerly known as (Awat Series).

These lithological units were extensively intruded by

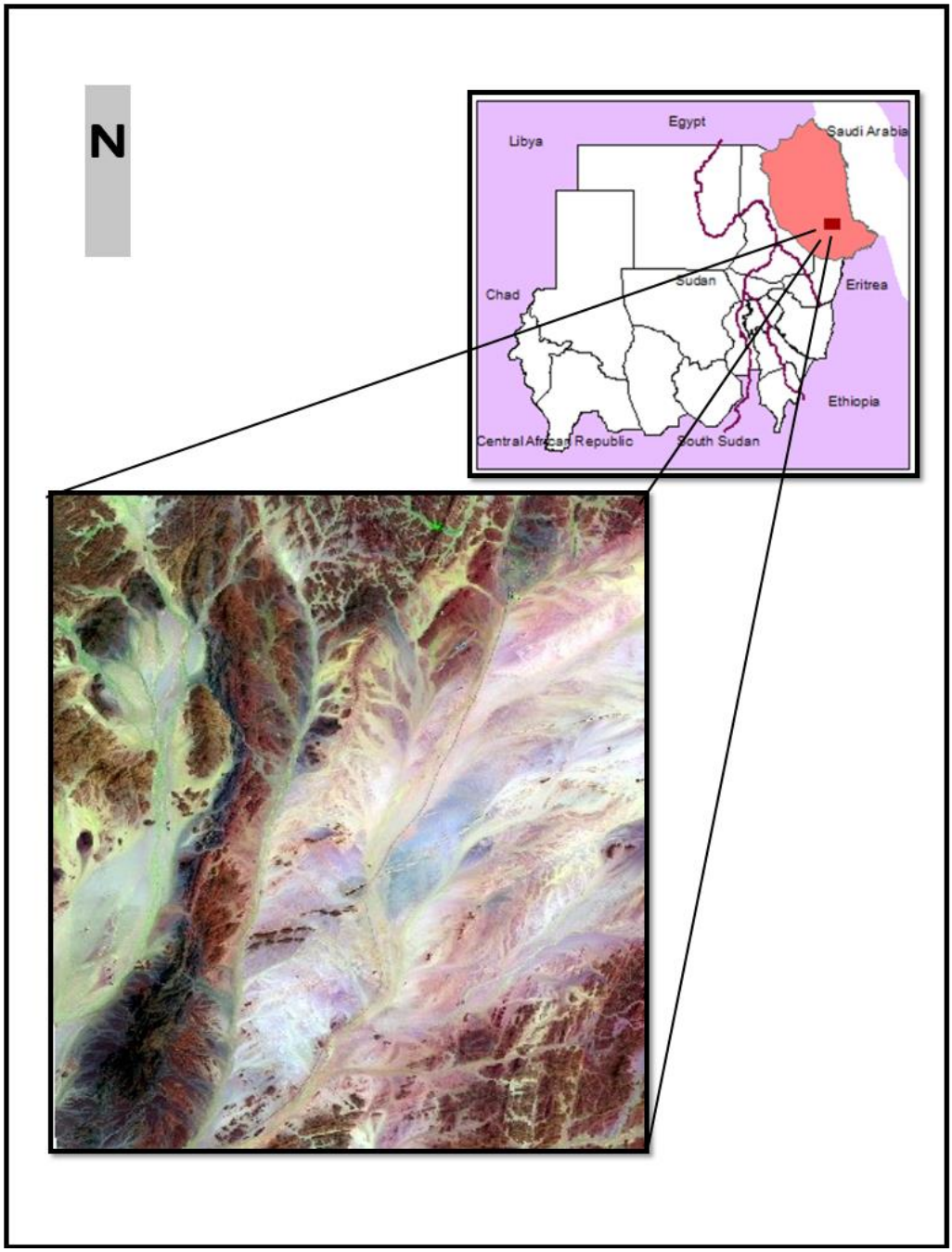

Figure 1. Location map of the study area.

plutonic rocks and placed at different times during the tectonomagmatic history of the basement complex of the Red Sea Hills (Kroner *et al*., 1987; Vail, 1988).

The igneous intrusive rocks cover about 50% of the total area of the RSH terrains. They vary in mode of occurrence from huge batholiths to stocks and plugs. Ring complexes and dyke swarms are common. Intrusive of the RSH terrains emplaced at different times during the Pan-African orogeny. The Nubian Shield is dominated by volcanogenic sediments metamorphosed in schist greenschist facies. These rocks comprise arc volcanics, associated intrusive rocks, immature sediments, and ophiolitic remnants of arc- and back-arc basins (Kroner *et al*., 1987; Vail, 1988). This shield itself is divided into five intra-oceanic and island-arc terranes, separated by sutures and shear zones; these five terranes, from north to south, are Gerf, Gabgaba, Gebeit, Haiya, and Tokar (Johnson *et al*., 2003; Blasband, 2006). The exploration geologist pays more attention to hydrother-

mally altered rocks and clay minerals because of their potential economic importance and diagnostic spectral features as a key for their identification via remote sensing techniques (Pour and Hashim, 2011).

METHODOLOGY

The present investigations are based on digital image processing of remotely sensed data combined with GIS spatial analysis and cartography manipulation. Very few fieldwork data have been manipulated to Identify hydrothermal alteration mapping using spectral analysis of ASTER Data. A laboratory–office digital image processing and GIS investigation were utilized as the main approaches for this study to check the obtained exploration results.

The spectral semi-hyperspectral ASTER data

ASTER sensor is one of the five state-of-the-art instrument sensor systems onboard Terra, a satellite launched in December 1999 by NASA, and state-of-the-art instrument sensor systems on board Terra, a satellite launched in December 1999 by NASA and the Japanese Ministry of International Trade and Industry. The ASTER system (Advanced Space Borne Thermal Emission and Reflection Radiometer) has 14 bands. It is a zoom lens for their instrument aboard Terra because it has the highest resolution orbital sensor system. The platform is described as a Sun-synchronous. Spectral bands and spatial resolution are generally more detailed than those of Landsat, meaning it is particularly useful for geological studies to identify mineral groups such as clays, carbonates, silica, iron-oxides and other silicates, and environmental monitoring, vegetation, hazard monitoring, soils, land surface, climatology, hydrology, and land cover change. However, unlike Landsat, repeat coverage by the ASTER sensor is more frequent and consists of three separate instrument subsystems; there are three groups of channels: Visible and Near Infrared (VIR) incorporates three spectral bands with 15m resolution, the Short-Wave Infrared (SWIR) operates in six spectral bands that provide 30 m resolution and the Thermal Infrared (TIR) operates in five bands in the thermal region with a resolution of 90 m. All ASTER bands cover the same 60 Km imaging swath with a pointing capability in a cross-track direction to cover 116 Km from Nadir at an altitude of 705 Km. The scan angle is 98.3°. This is accessible at least once every 16 days (http://speclab.cr.usgs.gov). ASTER high-resolution satellite capable of producing stereo imagery for creating detailed digital terrain models (DTMs) and the generation of digital elevation models (DEMs) (https;//search. earthdata.nasa.gov/search) (Tables 1 and 2). The study area covered one scene of ASTER image to study specific alteration zones area, which has been downloaded from the USGS official website (www.Earthexplorer.org) and subset this scene acquired as a separate file in Geotiff format.

The use of ASTER data in mineral prospecting has increased in recent years because of its relatively low cost, broad coverage, and unique integral bands susceptible to alteration minerals. The visible near-infrared (VNIR) and wave short-wave infrared (SWIR) portions of the spectrum are powerful geology tools as they cover many minerals' key absorption features. One of the main aims of geological remote sensing has been the development of methods for mineral mapping and rock-type discrimination. The USGS data set is a spectral database, a spectral database; many samples are gathered from different localities with different ingredients. This variety results in slight chemical differences in the sample, yielding different intensities in reflectance or even resulting in different spectral curves. Another spectral library is the JPL spectral library; this includes laboratory reflectance spectra of 160 minerals in digital form over the wavelength range from 0.4 to 2.5 μm (http://speclib.jpl.nasa.gov). Spectral analysis of the hyperspectral data aimed to compare and match the spectral curve of a particular mineral, rock, and material with a standard curve for similar standard objects. Common spectral libraries contain laboratory data for different standard minerals, rocks, soil, plants, and objects, such as the USGS, JHP, and Jet Propulsion libraries. Hydrothermally altered zones map produced by index minerals extracted from spectral analysis and resampled with aster image of the study area. After that, these results will be compared with those of the USGS spectral library.

The research focuses on extracting endmembers and using them to create abundance images for individual materials using a partial unmixing technique such as MTMF. The abundance of the different end members is estimated using matched filtering. The matching of abundance images by reducing false positives is done using feasibility scores ranging from 0 to 1. The feasibility scores define the non-probability of the abundance of a particular target in the pixel addition of the target spectra and the background spectra. The methodology is involved in the following processing sequence: (a) preprocessing of the data to prepare the dataset for further processing, (b) dimensionality reduction of the data (MNF transformation), (c) estimation of the spectral endmembers, (d) identification and comparison of the endmembers selected by visual inspection with automatic identification and spectral library, and (e) generation of a material map using the MTMF approach (Figure 2).

RESULTS AND DISCUSSIONS

Remote sensing data processing of the ASTER data analysis

In this study, the optical VNIR and SWIR data have been resampled together as nine bands of semi-hyperspectral data. These pre-processing techniques include correction

Table 1. Remote sensing image for the study.

Area of interest ASTER image	Resolution 15 m
AST_L1T_00303192002081459-20150421221219_4700.tif, acquisition date: March 19th, 2002	

Table 2. Specification of ASTER data.

Band	Spectral Range (μm)	Region	Spatial Resolution
Band 1	0.52-0.60		
Band 2	0.63-0.69	VINR	15 M
Band 3	0.76-0.86		
Band 4	1.60-1.70		
Band 5	2.145-2.185		
Band 6	2.185-2.225	SWIR	30 M
Band 7	2.235-2.285		
Band 8	2.295-2.365		
Band 9	2.360-2.430		
Band 10	8.125-8.475		
Band 11	8.475-8.825		
Band 12	8.925-9.275	TIR	90 M
Band 13	10.25-10.95		
Band 14	10.95-11.65		

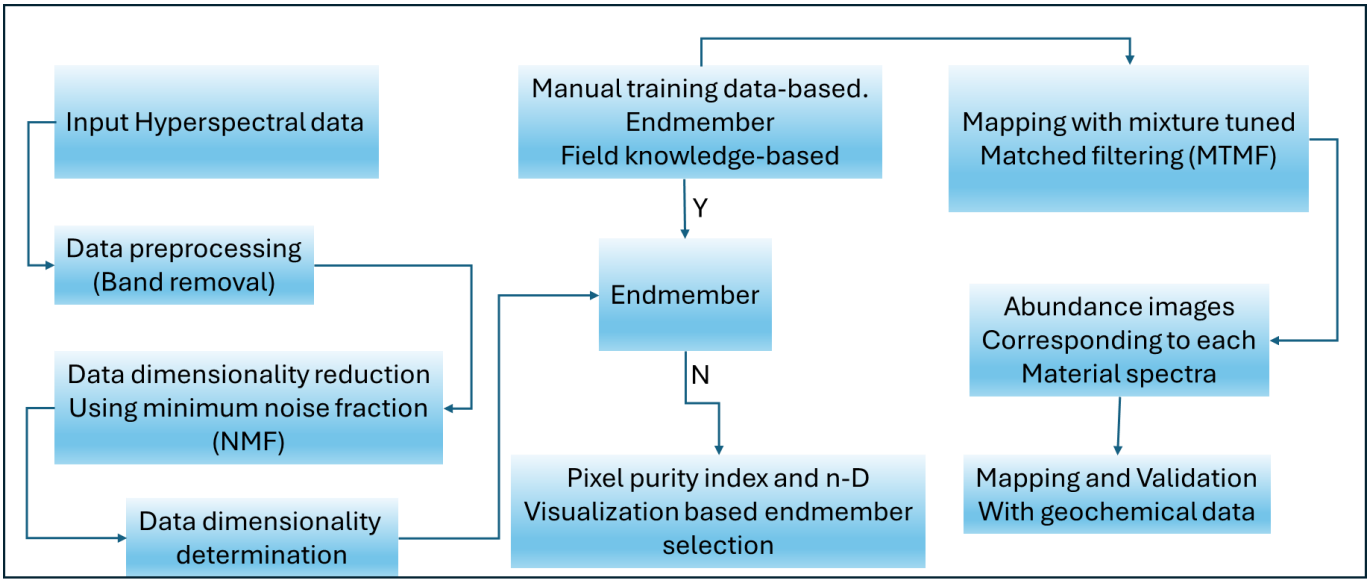

Figure 2. Flowchart of image processing and MTMF-based mapping steps.

of image and layer stacking of VNIR-SWIR. Moreover, converting pixel radiance at the sensor into reflectance at surface data using the FLAASH module (Figure 3). The USGS laboratory spectra used in this study are grouped according to alteration assemblages and include the following:

1. Alunite and kaolinite, typical constituents in argillic alteration absorption, feature at 2.20 and 2.17, at 2.20 and 2.17 μm (ASTER band 5).
2. Chlorite and malachite are associated with propylitic alteration and display absorption peaks at 2.31–2.33 μm absorption features (ASTER band 8).

Figure 3. The spatial extent of ASTER Sub-Scene with respect to study Spectral analysis.

3. Muscovite and illite, typical in phyllic alteration, with a 2.20 µm absorption feature (ASTER band 6)
4. Hematite, which is typical in Oxidation (Fe) alteration. To facilitate the spectral analysis, the USGS spectral library of alunite, chlorite, hematite, illite, kaolinite, malachite, and muscovite minerals were resampled to ASTER AVNIR-SWIR spectra (Figure 4a and b).

Moreover, the ASD TerraSpec Halo device measured the spectral measurements of samples from the study area for the chlorite, epidote, illite, biotite, and phenacite minerals and resamples for ASTER AVNIR-SWIR spectra (Figure 4c and d). Minerals were identified through analysis and compared with the results of the USGS spectral library, which were then converted into digital data for spatial analysis using geographic information systems (GIS).

This study aligns with previous research conducted in various regions worldwide, e.g., Yalcin *et al*. (2020) in the Akarcay Basin of Turkey, Honarmand *et al.* (2013) in the Kerman magmatic arc of Iran, Saravia (2021) in Peru, Abubakar *et al*. (2019) in West Africa, Nigeria, Abdelouhed *et al.* (2021) in Morocco, Wang *et al*. (2020) in China, and El-Desoky *et al*. (2021, 2022) in Egypt.

Mixture Tuned Matched Filtering (MTMF)

The mixture-tuned matched Filtering (MTMF) is one algorithm of the spectral analysis applied during the present study. The MTMF is a hybrid method based on a combination of well-known signal–processing methodologies and linear mixture theory. This method benefits the ability to map a single known target without the knowledge of all end member's signatures, with the leverage of mixed pixel models, including placing constraints on feasibility. MTMF suppresses background

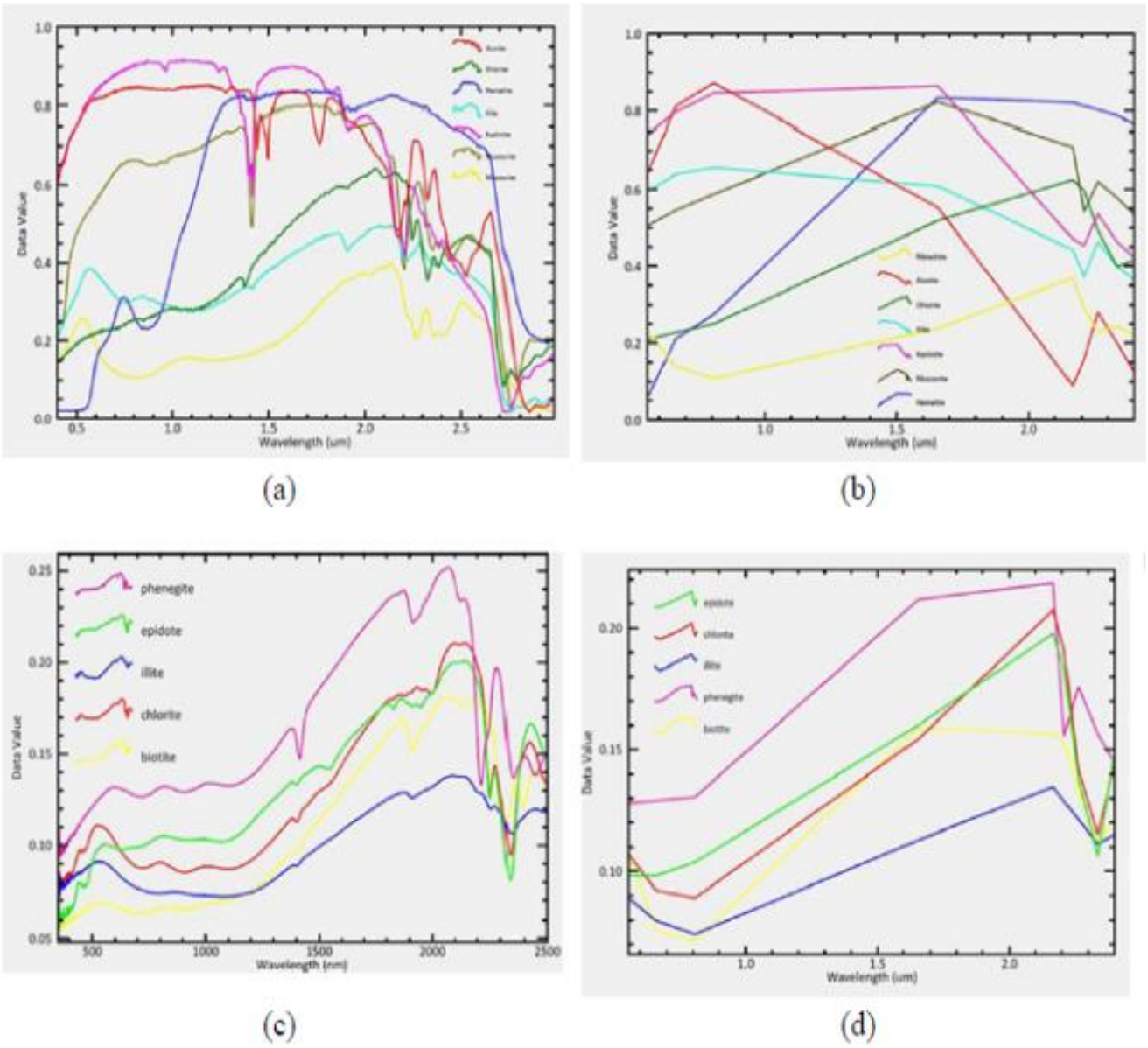

Figure 4. Spectral library profiles with ASTER data, (a) The USGS Spectral library for the alteration minerals, (b) the USGS Spectral Curves after resampled with ASTER image for the study area for alunite, chlorite, hematite, illite, kaolinite, malachite, and muscovite. (c) Spectral Curves Measured by (ASD TerraSpec Halo) device for the study area for the chlorite, epidote, illite, Biotite and phenegite before resampled. (d) Spectral Curves Measured by (ASD TerraSpec Halo) device for the study area for the chlorite, epidote, illite, Biotite, and phenacite after resampled.

noise and estimates the pixel sub-pixel abundance of a single target material (Honarmand *et al*., 2013). The MTMF method includes the following steps:

1. MNF transformation of apparent reflection data.
2. Matched filtering for abundance estimation and mixture tuning to identify infeasible or false-positive pixels.

The MTMF algorithm was applied to nine (VNIR-SWIR bands) ASTER data to identify identical minerals in the alteration zones associated with known porphyry copper deposits in the study area. The MTMF algorithm combines the best parts of the linear spectral mixing model and the statistically Matched Filter Model. Figure 5 shows that Chlorite, Epidote, Illite, Phenegite, and Biotite are identified using different thresholds for mineral alteration, with Chlorite in red, Epidote in green, Illite in blue, Phenegite in magenta, and Biotite in yellow.

This study's (Mixture Tuned Matched Filtering) results align with previous studies by Muavhi (2022), Yousefi *et al.* (2018), and Ayoobi and Tangestani (2017), which used the

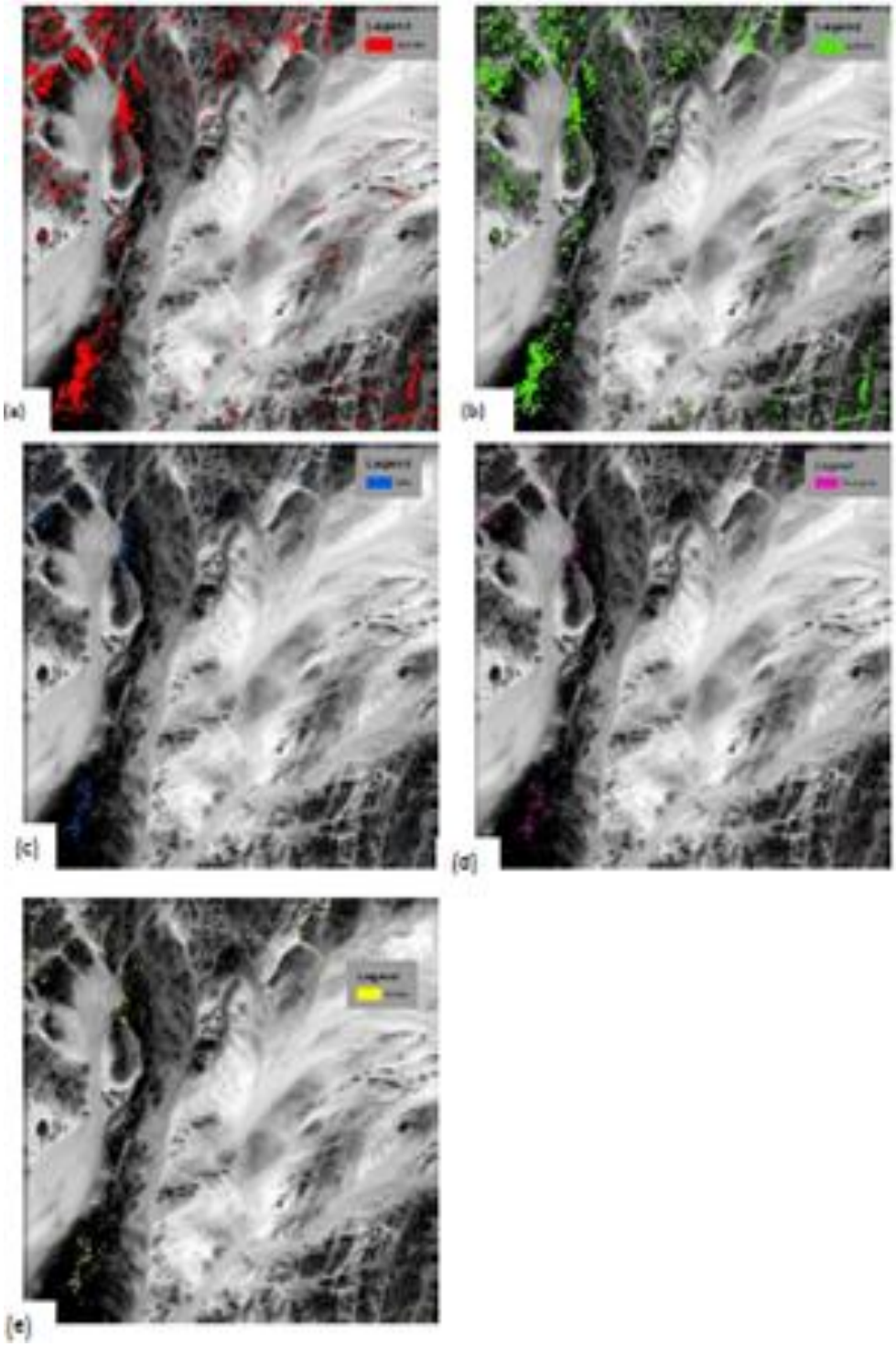

Figure 5. The results of the MTMF Classifier for alteration minerals: (a) chlorite appears in the red, (b) epidote appears in the green, (c) illite appears in the blue, (d) phenegite appears in the magenta, and (e) Biotite appears in the yellow minerals mapping using threshold 0.22, 0.21, 0.23, 0.24 and 0.24, respectively.

method on ASTER images to map hydrothermal alterations in highly metamorphosed terrain in the Musina copper deposit field, Porphyry Cu Deposits in Jabal-Barez Ranges, Kerman Copper Belt of Iran, and evaluated the effect of spatial subsetting using ASTER over hydrothermally altered terrain.

Table 3. Alterations types found in the study area.

Alteration types	Representing minerals
potassic	Biotite, Muscovite
propylitic	Epidote, Chlorite
Phyllic or sericitic	Illite, Phenegite

Table 4. Chemical analysis for trace elements of the study area.

Sample No.	Au (ppm)	Pb (ppm)	Cu (ppm)	Co (ppm)	Zn (ppm)
HRS1A	0.022	14.7	36.6	6.2	56.1
HRS3	0.048	15.3	33.5	17.8	96.5
HRS4A	0.179	21.9	8.1	16.4	88.1
HRS4B	0.129	26.8	471.0	9.9	45.1
HRS5B	0.253	16.9	51.5	8.1	59.9
HRS6	0.231	23.7	153.0	24.7	91.5
HRS8	0.113	21.5	179.3	12.8	121.9
HRS9	0.100	22.0	178.8	23.0	117.7
HRS11A	0.134	19.0	40.9	30.3	111.1
HRS11B	0.338	21.5	52.2	27.9	87.6
HRS12	0.121	26.4	57.3	35.5	121.5
HRS13	0.117	21.8	8.0	28.4	65.1
HRS14	0.114	9.8	64.0	ND	33.9
HRS15	0.160	18.1	15.2	27.8	136.1

Spatial analysis of the spectral signatures of the MTMF classifier

The MTMF classifier images display the spatial distribution of minerals, which could be related to the alteration halos of the mineralization zones. The results rule images display the spatial distribution of the concerned mineral by its distinguishable absorption features beside the vector layer of the same rule image. The spectral and spatial analysis of ASTER data indicates probable alteration zones related to mineralization existed in the study area. The analysis focuses on the spatial distribution of the main types of hydrothermally altered minerals. The spectral analysis of ASTER data is based on the spectral signatures compared with laboratory and library spectra of these minerals. The obtained spectra of TerraSpec Halo mineral identifier (ASD) instruments provide spectra for chlorite and epidote. They are associated with propylitic alteration, phenacite, and Illite, typical minerals in phyllic or sericite alteration zones, while the biotite, muscovite, are typical in potassic alteration (Table 3 and Figure 6).

The spectral signature obtained from TerraSpec Halo mineral identifier (ASD) instruments was found to be in concordance with the USGS spectral library of alteration minerals. Hence, both were compared in the MTMF classifier and provided similar results (Figures 6 and 7). This result ascertains the advantages of utilizing the spectral analysis of hyperspectral data over the multispectral data in mineral exploration investigation in specifying the alteration zones related to mineralization.

Zhao *et al.* (2024) used the MTMF method for hydromagnesite determination using satellite data from the Jiezechaka Salt Lake in Tibet. Santos *et al*. (2022) applied the spectral unmixing method to PRISMA hyperspectral images to identify Li minerals. Hegab *et al*. (2022) analyzed remote sensing, geophysical, and GIS data for gold-related alteration zone detection in the Um Balad Area, Egyptian Eastern Desert. Kumar *et al.* (2022) assessed different spectral unmixing techniques on hyperspectral imagery. Using ASTER satellite data, Pour *et al*. (2020) identified phyllosilicates in Antarctic environments. Adiri *et al.* (2020) mapped mineralized zones using Landsat-8 OLI, Terra ASTER, and Sentinel-2A multispectral data. The above-mentioned researchers have used the Spatial analysis of the spectral signatures of the MTMF classifier, and their results validated the outcomes of the current study.

Geochemical evaluation

The outcome of the remote sensing and GIS investigations have been validated by ground thrusting to assess the delineated alteration zones. 14 alteration zone samples (Table 4) were used to delineate hydrothermally altered rocks located by the global position system (GPS). Alterations and Quartz vein samples were selected for Atomic Absorption Spectrometry (AAS) from the delineated

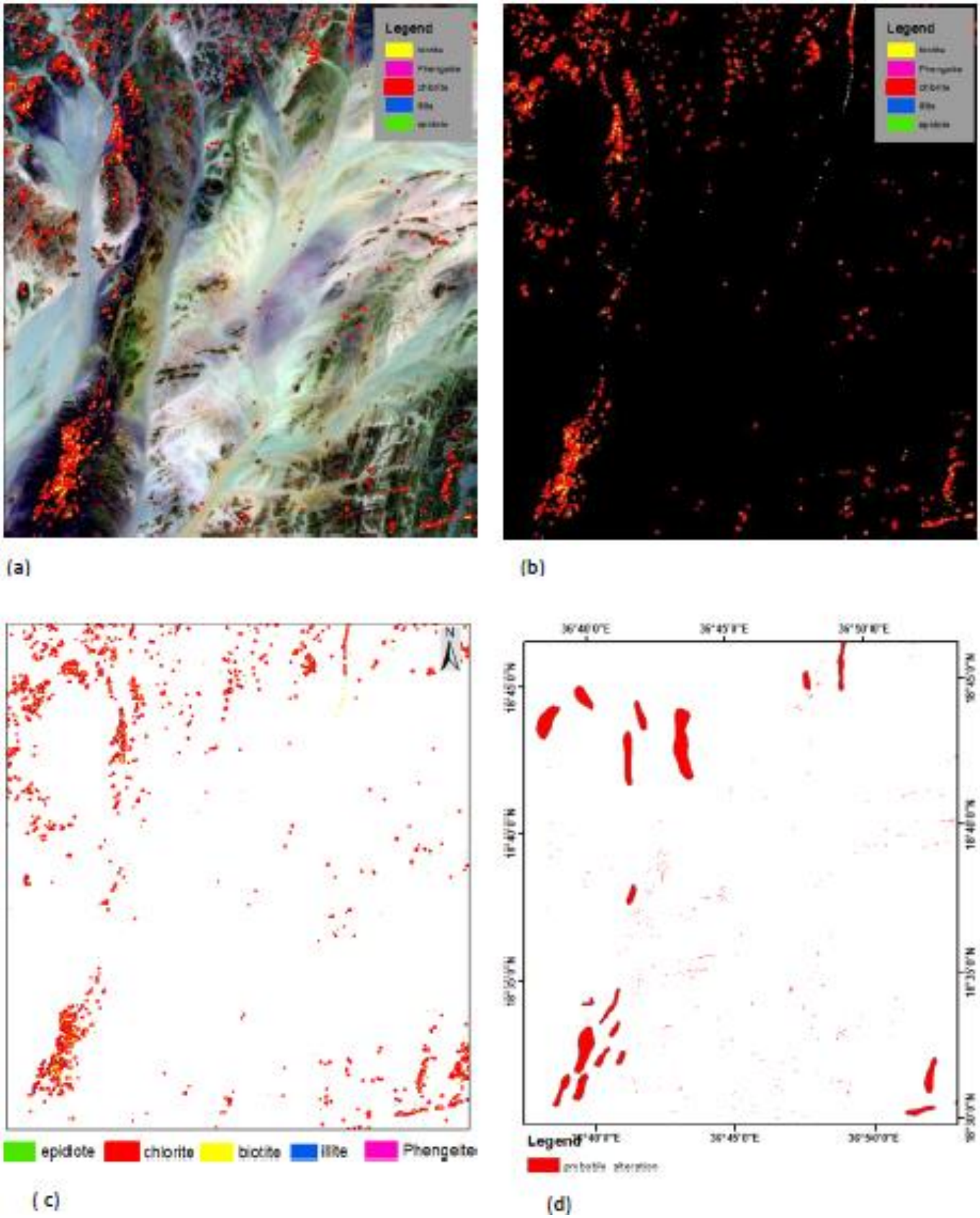

Figure 6. Combined minerals map produced by MTMF Classification for image of specified study area (a) combined minerals overlain the satellite image, (b & c) alteration minerals polygon in rule image. (d) combined potential alteration zone.

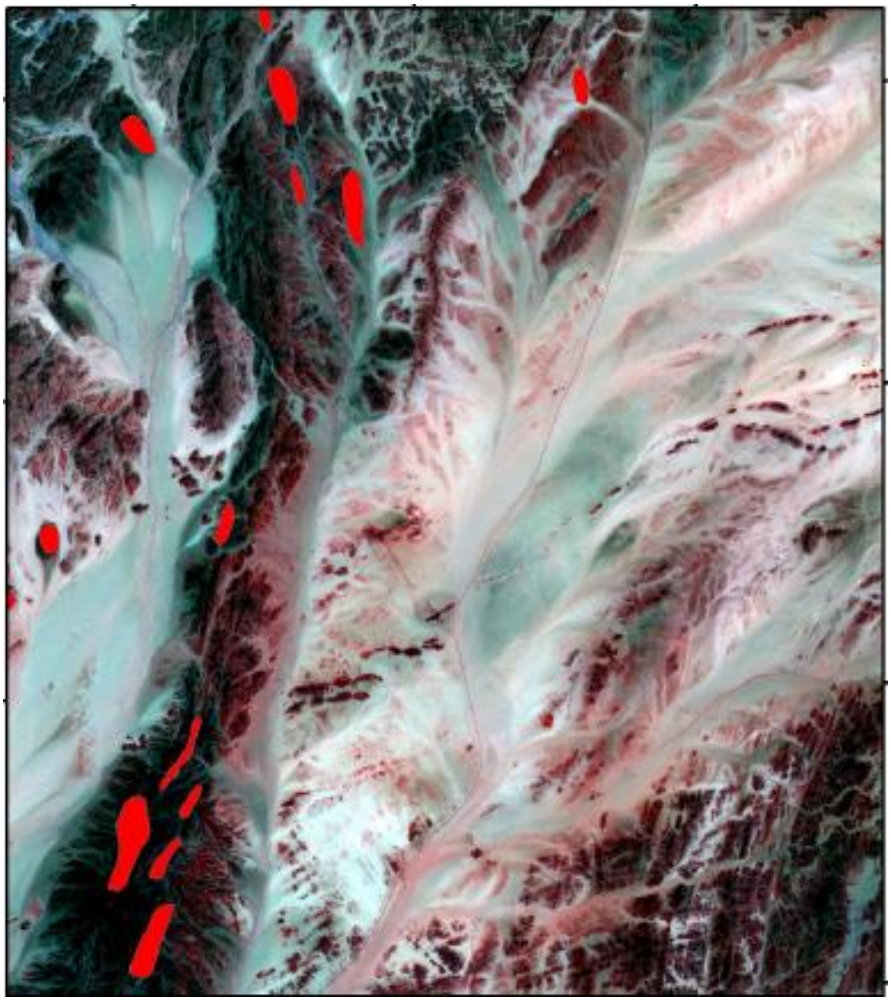

Figure 7. Probable alteration zones overlain ASTER subset data. The MTMF classifier spectrally analyzed the ASTER data with the mineral spectra of the USGS spectral library and ASD Terra SpectHallo Library. The red color depicted the probable alteration zones map related to mineralization resulted from the cumulative of alteration minerals.

hydrothermal veins. The obtained results are displayed in. These samples were taken from different areas. The results from the gold-bearing quartz veins and alteration zones show a clear variation in gold distribution. Gold concentrations range between 0.022 and 0.338 parts per million (ppm), with an average concentration between 0.022 and 0.048 ppm; these values are considered low from an economic perspective, as the minimum profitable threshold for gold extraction is typically between 0.5 and 1.0 ppm. The higher value found (0.338 ppm) is still below the economic threshold, but it indicates the potential presence of better mineralization in the area, warranting further exploration. The variation in gold distribution suggests that gold may be concentrated in local structural formations or specific areas within quartz veins and alteration zones. Remote sensing can guide fieldwork efforts toward potential zones, but chemical analysis remains crucial for evaluating the mineral potential. Further analysis at different depths of the outcome of the present study proved the effectiveness of using remote sensing methods in mineral exploration and delineation of hydrothermal alteration zones. Several studies (e.g., Eldosouky *et al*., 2024; Sikakwe, 2023; Alarifi *et al*., 2022; Mohamed *et al*., 2021; Zeinelabdein *et al.,* 2020; Shi *et al.,* 2020; Githenya *et al.,* 2019; Rokos *et al*., 2000) have adopted these methods. These methods have become more critical in mineral exploration, reducing fieldwork time and cost to determine if higher gold concentrations exist.

Conclusion and Recommendations

The study area is part of the crystalline basement of the Haiya terrain of the late Proterozoic age. It is dominated by

low–grade arc—and back-arc metavolcanic-sedimentary sequences decorated by dismembered ophiolitic belts and intruded by granitoid intrusions of different ages.

Digital image processing revealed the areas mentioned, the areas with favourable hydrothermal alteration signals that were later verified in the field. Geochemical analyses using portable XRF devices and atomic absorption spectrometry (AAS) analysis revealed the presence of alterations in the study area. The outcome of the present study indicated a high potential for alterations in the area. The digital image processing of the fused semi-hyperspectral of Aster data is directed to produce alterations to the zone map. Spectral analysis ASTER semi-hyperspectral data were utilized to delineate the map of the alteration zones related to mineralization employing the spectral signatures of their minerals. The Spectral Mapping MTMF classifier of ASTER semi-hyperspectral data provided more details of alteration halos related to mineralization zones. The cumulative images of the MTMF results portray the highly probable results of chemical and spectral analysis of minerals. Remote sensing techniques should be integrated with fieldwork and laboratory analysis to enhance the accuracy of mineral detection and confirm results with lower costs and higher reliability. Therefore, the following are recommended:

- Additional exploration techniques, such as geophysical surveys (magnetic or electrical resistance methods), can be utilized to identify subsurface structures that might contain higher concentrations of gold.
- Multispectral and hyperspectral data are recommended to improve the accuracy of mineral identification and, more precisely, determine alteration types.
- To improve the results of remote sensing digital image processing, more detailed geological fieldwork and structural analysis in the region and their relation to mineralization need to be carried out in the future.

CONFLICT OF INTEREST

The authors declare they have no conflict of interest.

ACKNOWLEDGMENTS

The authors would like to thank all teachers and colleagues of the M. Sc. Batch II: Applications of Remote Sensing and GIS in Geology for their valuable information, support, and encouragement; we also acknowledge the Geological Research Authority of Sudan (GRAS) for their endless encouragement and support. We would also like to acknowledge the Department of Geology, Faculty of Petroleum and Minerals, Al Neelain University, for their help and support.

REFERENCES

Abdel Rahman, E. M. (1993). *Geochemical and geotectonic controls of the metallogenic evolution of selected ophiolite complexes from the Sudan* (Vol. 145). Reimer.

Abdelouhed, F., Algouti, A., Algouti, A., Mohammed, I., & Mourabit, Z. (2021). Contribution of GIS and remote sensing in geological mapping, lineament extractions and hydrothermal alteration minerals mapping using ASTER satellite images: case study of central Jebilets-Morocco. *Disaster Advances*, *14*(1), 15-25.

Abdelsalam, M. G., Stern, R. J., Schandelmeier, H., & Sultan, M. (1995). Deformational history of the Neoproterozoic Keraf Zone in NE Sudan, revealed by shuttle imaging radar. *The Journal of Geology*, *103*(5), 475-491.

Abubakar, A. J. A., Hashim, M., & Pour, A. B. (2019). Identification of hydrothermal alteration minerals associated with geothermal system using ASTER and Hyperion satellite data: a case study from Yankari Park, NE Nigeria. *Geocarto International*, *34*(6), 597-625.

Adiri, Z., El Harti, A., Jellouli, A., Maacha, L., Azmi, M., Zouhair, M., & Bachaoui, E. M. (2020). Mineralogical mapping using landsat-8 OLI, terra ASTER and sentinel-2A multispectral data in Sidi flah-bouskour inlier, Moroccan anti-atlas. *Journal of Spatial Science*, *65*(1), 147-171.

Alarifi, S. S., Abdelkareem, M., Abdalla, F., Abdelsadek, I. S., Gahlan, H., Al-Saleh, A. M., & Alotaibi, M. (2022). Fusion of multispectral remote-sensing data through GIS-based overlay method for revealing potential areas of hydrothermal mineral resources. *Minerals*, *12*(12), 1577.

Ali, E. (2005). The Geology and Structural Evolution of the Area Around the River Nile Between Atbara and Abidiya, Nile State, Sudan. *Remote Sensing, Structural and Geochemical Approaches. MSc thesis, Al Neelain University*.

Ayoobi, I., & Tangestani, M. H. (2017). Evaluating the effect of spatial subsetting on subpixel unmixing methodology applied to ASTER over a hydrothermally altered terrain. *International Journal of Applied Earth Observation and Geoinformation*, *62*, 1-7.

Babikii, I. A. A. (2006). *Digital Image Processing of Landsat7 data and GIS Application for Geological Investigation in Jebel Erba Area, Red Sea Hills, NE Sudan A* (Doctoral dissertation, Neelain University).

Bakor, A. R., Gass, I. G., & Neary, C. R. (1976). Jabal al Wask, northwest Saudi Arabia: an Eocambrian back-arc ophiolite. *Earth and Planetary Science Letters*, *30*(1), 1-9.

Blasband, B. B. (2006). *Neoproterozoic Tectonics of the Arabian-Nubian Shield* (Vol. 256). Ph. D. Thesis, Utrecht University.

Boardman, J. W., & Kruse, F. A. (2011). Analysis of imaging spectrometer data using $ n $-dimensional geometry and a mixture-tuned matched filtering approach. *IEEE Transactions on Geoscience and Remote Sensing*, *49*(11), 4138-4152.

Camp, V. E. (1984). Island arcs and their role in the evolution of the western Arabian Shield. *Geological Society of America Bulletin*, *95*(8), 913-921.

Chen, Q., Zhao, Z., Zhou, J., Zhu, R., Xia, J., Sun, T., Zhao, X., & Chao, J. (2022). ASTER and GF-5 satellite data for mapping hydrothermal alteration minerals in the longtoushan Pb-Zn deposit, SW China. *Remote Sensing*, *14*(5), 1253.

El Khidir, S. O. (2006). Remote sensing and GIS applications in geological mapping, prospecting for mineral deposits and Groundwater-Berber sheet area, northern Sudan. Ph.D. thesis, Al Neelain University, Khartoum, Sudan.

El Khidir, S. O., & Babikir, I. A. (2013). Digital image processing

and geospatial analysis of Landsat 7 ETM+ for mineral exploration, Abidiya area, North Sudan. *International Journal of Geomatics and Geosciences*, *3*(3), 645-658.

El-Desoky, H. M., Soliman, N., Heikal, M. A., & Abdel-Rahman, A. M. (2021). Mapping hydrothermal alteration zones using ASTER images in the Arabian–Nubian Shield: A case study of the northwestern Allaqi District, South Eastern Desert, Egypt. *Journal of Asian Earth Sciences: X*, *5*, 100060.

El-Desoky, H. M., Tende, A. W., Abdel-Rahman, A. M., Ene, A., Awad, H. A., Fahmy, W., El-Awny, H., & Zakaly, H. M. (2022). Hydrothermal alteration mapping using landsat 8 and ASTER data and geochemical characteristics of Precambrian rocks in the Egyptian shield: A Case Study from Abu Ghalaga, Southeastern Desert, Egypt. *Remote Sensing*, *14*(14), 3456.

Eldosouky, A. M., Eleraki, M., Mansour, A., Saada, S. A., & Zamzam, S. (2024). Geological controls of mineralization occurrences in the Egyptian Eastern Desert using advanced integration of remote sensing and magnetic data. *Scientific Reports*, *14*(1), 16700.

Elsayed Zeinelabdein, K. A., (2002). Application of remote sensing in geological mapping, hydrogeological investigation and mineral exploration, Red Sea Hills northeastern Sudan. M. Sc. Thesis. Department of Geology, University of Khartoum, Sudan.

Fitches, W. R., Graham, R. H., Hussein, I. M., Ries, A. C., Shackleton, R. M., & Price, R. C. (1983). The late Proterozoic ophiolite of Sol Hamed, NE Sudan. *Precambrian Research*, *19*(4), 385-411.

Githenya, L. K., Kariuki, P. C., & Waswa, A. K. (2019). Application of remote sensing in mapping hydrothermal alteration zones and geological structures as areas of economic mineralization in Mwitika-Makongo Area, SE Kenya. Journal of Environment and Earth Science, 9(11), 16-27.

Hegab, M. A. E. R., Mousa, S. E., Salem, S. M., Farag, K., & GabAllah, H. (2022). Gold-related alteration zones detection at the Um Balad Area, Egyptian Eastern Desert, using remote sensing, geophysical, and GIS data analysis. *Journal of African Earth Sciences*, *196*, 104715.

Honarmand, M., Ranjbar, H., & Shahabpour, J. (2013). Combined use of ASTER and ALI data for hydrothermal alteration mapping in the northwestern part of the Kerman magmatic arc, Iran. *International Journal of Remote Sensing*, 34(6), 2023-2046.

Johnson, P. R., Abdelsalam, M. G., & Stern, R. J. (2003). The Bi'r Umq-Nakasib suture zone in the Arabian-Nubian shield: a key to understanding crustal growth in the East African orogen. *Gondwana Research*, *6*(3), 523-530.

Kenea, N. H. (1997). Digital image processing and GIS data integration for geological studies in the Red Sea Hills, Sudan. Ph. D. Thesis. Free University of Berlin. Germany.

Kroner, A., Greiling R., Reichmann T., Hussein I. M., Stern. R. J, Dürr. S, Kruger. R and. Zimmer, M (1987). "Pan-African crustal evolution in the Nubian segment of Northeast Africa. In: Kroner, A. (ed.). *Proterozoic Lithosphere Evolution*. Geodynamics Series, International Lithosphere Program contribution. American Geophysical Union, Washington. Pp. 235-257.

Kumar, V., Pandey, K., Panda, C., Tiwari, V., & Agrawal, S. (2022). Assessment of Different Spectral Unmixing Techniques on Space Borne Hyperspectral Imagery. *Remote Sensing in Earth Systems Sciences*, *5*(3), 129-140.

Mehr, S., Ahadnejad, V., Abbaspour, R. A., & Hamzeh, M. (2013). Using the mixture-tuned matched filtering method for lithological mapping with Landsat TM5 images. International Journal of remote sensing, *34*(24), 8803-8816.

Mohamed, M. T. A., Al-Naimi, L. S., Mgbeojedo, T. I., & Agoha, C. C. (2021). Geological mapping and mineral prospectivity using remote sensing and GIS in parts of Hamissana, Northeast Sudan. *Journal of Petroleum Exploration and Production*, *11*(3), 1123-1138.

Mohammed, A. A. B., & El Khidir, S. O. H. (2023). The use of Landsat 8 OLI image for the delineation of hydrothermal alterations zones in the Haiya Area, Red Sea Hills, NE Sudan. *International Journal of Social Relevance and Concern*, *11*(11), 1-9.

Muavhi, N. (2022). Application of per-pixel and sub-pixel unmixing methods on ASTER images to map hydrothermal alterations in a highly metamorphosed terrain: a case of the Musina copper deposit field. Geocarto International, 37(26), 13579-13595.

Neary, C. R., Gass, I. G., & Cavanagh, B. J. (1976). Granitic association of northeastern Sudan. Bull. GSA Bulletin, 87(10), 1501-1512.

Pour, A. B., Sekandari, M., Rahmani, O., Crispini, L., Läufer, A., Park, Y., Hong, J. K., Pradhan B., Hashim M., Hossain M. S., Muslim A. & Mehranzamir, K. (2020). Identification of phyllosilicates in the antarctic environment using ASTER satellite data: case study from the Mesa Range, Campbell and Priestley Glaciers, Northern Victoria Land. *Remote Sensing*, *13*(1), 38.

Pour, B. A., & Hashim, M. (2011): Spectral transformation of ASTER and the discrimination of hydrothermal alteration minerals in a semi-arid region, SE Iran. *International Journal of the Physical Sciences*, *6*(8), 2037-2059.

Rajendran, S., & Nasir, S. (2017). Characterization of ASTER spectral bands for mapping of alteration zones of volcanogenic massive sulphide deposits. *Ore Geology Reviews*, *88*, 317-335.

Rokos, D., Argialas, D., Mavrantza, R., St.-Seymour, K., Vamvoukakis, C., Kouli, M., Lamera, S., Paraskevas H., Karfakis, I., & Denes, G. (2000). Structural analysis for gold mineralization using remote sensing and geochemical techniques in a GIS environment: island of Lesvos, Hellas. *Natural Resources Research*, *9*(4), 277-293.

Saad, E. A., Abdellsamed, I. M., Dawelbeit A., Wadi, D., & Ahmed A. H. (2024). The analysis of Landsat 8 OLI image for delineation of hydrothermal alteration zones in the Artoli Area, Berber Province, Northern Sudan. *Global Journal of Earth and Environmental Science*, *9*(3), 87-97.

Santos, D., Cardoso-Fernandes, J., Lima, A., & Teodoro, A. C. (2022, October). The potential of spectral unmixing method applied to PRISMA hyperspectral images in the identification of Li minerals: an evaluation for prospecting purposes. In *Earth Resources and Environmental Remote Sensing/GIS Applications XIII* (Vol. 12268, pp. 257-271). SPIE.

Saravia, J. A. (2021). Identification of patterns associated with areas of epithermal alteration through responses spectral using ASTER images. *The Egyptian Journal of Remote Sensing and Space Science, 24*(3), 353-360.

Shi, X., Al-Arifi, N., Abdelkareem, M., & Abdalla, F. (2020). Application of remote sensing and GIS techniques for exploring potential areas of hydrothermal mineralization in the central Eastern Desert of Egypt. *Journal of Taibah University for Science*, *14*(1), 1421-1432.

Siddiqui, A., Chauhan, P., Kumar, V., Jain, G., Deshmukh, A., & Kumar, P. (2022). Characterization of urban materials in AVIRIS-NG data using a mixture tuned matched filtering (MTMF) approach. *Geocarto International*, *37*(1), 332-347.

Sikakwe, G. U. (2023). Mineral exploration employing drones, contemporary geological satellite remote sensing and geographical information system (GIS) procedures: A review. *Remote Sensing Applications: Society and Environment*, *31*, 100988.

Vail, J. R. (1979). Outline of geology and mineralization of the Nubian Shield east of the Nile Valley, Sudan. *King Abdulaziz University Jeddah, Saudi Arabia, Institute of Applied Geology Bulletin, 3*, 97-107.

Vail, J. R. (1983). Pan-African crustal accretion in North–East Africa. *Journal of African Earth Science, 1*(3-4), 285-294.

Vail, J. R. (1985). Pan - African (late Precambrian) tectonic terrains and the reconstruction of the Arabian-Nubian shield. *Geology, 13*, 839-842.

Vail, J. R. (1976 b). Outline of the geochronology and tectonic units of the basement complex of Northeast Africa. *Proceedings Royal Society*, London A 350, 127–141.

Vail, J. R., (1988). “Tectonics and evolution of the Proterozoic basement of north-eastern Africa. In: El Gaby, S., & Greiling, R. (eds.). *The Pan-African Belt of Northeast Africa and adjacent areas*. F. Vieweg: Braunschweig. Pp. 195-226.

Wadi, D., Wu, W., & Fuad, A. (2021, October). Rock discontinuities mapping with computer-based lineament extraction from satellite imagery. In *IOP Conference Series: Earth and Environmental Science* (Vol. 861, No. 5, p. 052060). IOP Publishing.

Wang, Z., Zhou, C., & Qin, H. (2020). Detection of hydrothermal alteration zones using ASTER data in Nimu porphyry copper deposit, south Tibet, China. Advances in Space Research, 65(7), 1818-1830.

Yalcin, M., Kilic Gul, F., Yildiz, A., Polat, N., & Basaran, C. (2020). The mapping of hydrothermal alteration related to the geothermal activities with remote sensing at Akarcay Basin (Afyonkarahisar) will be done using Aster data. Arabian Journal of Geosciences, *13*(21), 1166.

Yousefi, S., Yousefi, E., Takahashi, H., Hayashi, T., Tampo, H., Inoda, S., ... & Asbell, P. (2018). Keratoconus severity identification using unsupervised machine learning. *PLoS One*, *13*(11), e0205998.

Zeinelabdein, K. A. E., El-Nadi, A. H. H., & Babiker, I. S. (2020). Prospecting for gold mineralization with the use of remote sensing and GIS technology in North Kordofan State, central Sudan. *Scientific African*, *10*, e00627.

Zhao, T., Dai, J., Zhao, Y., & Ye, C. (2024). MTMF method for hydromagnesite determination based on Landsat8 and ZY1-02D Data: A Case Study of the Jiezechaka Salt Lake in Tibet. *Aquatic Geochemistry*, 130, 219-238.